

Diagonal Antiferromagnetic Easy Axis in Lightly Hole Doped $\text{Y}_{1-x}\text{Ca}_x\text{Ba}_2\text{Cu}_3\text{O}_6$

András Jánossy,^{1,*} Titusz Fehér,^{1,2} and Andreas Erb³

¹*Institute of Physics, Budapest University of Technology and Economics,*

and Solids in Magnetic Fields Research Group of the Hungarian Academy of Sciences, P.O. Box 91, H-1521 Budapest, Hungary

²*Institute of Physics of Complex Matter, EPFL, CH-1015 Lausanne, Switzerland*

³*Walther Meissner Institut, Bayerische Akademie der Wissenschaften, D-85748 Garching, Germany*

(Dated: June 21, 2017)

Hole induced changes in the antiferromagnetic structure of a lightly Ca doped $\text{Gd:Y}_{1-x}\text{Ca}_x\text{Ba}_2\text{Cu}_3\text{O}_6$ copper oxide single crystal with $x \approx 0.008$ is investigated by Gd^{3+} electron spin resonance. Holes do not localize to Ca^{2+} ions above 2.5 K since the charge distribution and spin susceptibility next to the Ca^{2+} are independent of temperature. Both hole doped and pristine crystals are magnetically twinned with an external magnetic field dependent antiferromagnetic domain structure. Unlike the undoped crystal, where the easy magnetic axis is along [100] at all temperatures, the easy direction in the hole doped crystal is along the [110] diagonal at low temperatures and changes gradually to the [100] direction between 10 K and 100 K. The transition is tentatively attributed to a magnetic anisotropy introduced by hole ordering.

PACS numbers: 74.72.Bk, 75.25.+z, 75.50.Ee, 76.30.Kg

Keywords: antiferromagnetic domains, antiferromagnetic easy axis, hole localization, stripes

The structure of the magnetic elementary cell is well established in $\text{YBa}_2\text{Cu}_3\text{O}_6$, the antiferromagnetic (AF) parent compound of a high temperature superconductor, but little is known about how introducing holes affects the magnetic structure. Neutron diffraction found a chessboard like AF order in the basal (a, b) plane [1] which, in high purity crystals, alternates along the c direction with the periodicity of the lattice as shown in Fig. 1(a). In $\text{YBa}_2\text{Cu}_3\text{O}_{6+\delta}$ no hole induced change of this structure has been reported up to date. However, in $\text{La}_{2-x}\text{Sr}_x\text{CuO}_4$, the other well studied AF parent compound for high T_c superconductivity, hole doping changes the magnetic structure in a peculiar way [2, 3]. At low temperatures a static magnetic modulation appears with a wavelength roughly proportional to the hole concentration and is characterized by a single wavevector running

along one of the diagonals of the slightly distorted square CuO_2 lattice. It is not yet clear whether this spin density wave is or is not a manifestation of a theoretically predicted [4, 5] phase separation into hole-rich and undoped regions. Tranquada *et al.* [6] suggested that the stripe like charge and magnetic order in $\text{La}_{1.6-x}\text{Nd}_{0.4}\text{Sr}_x\text{CuO}_4$ and related compounds is evidence for such a phase separation. Ando *et al.* [7] interpreted the doping dependence of the resistivity in terms of segregated conducting stripes of holes. However, to present, electron structural studies [8] do not show the expected quasi 1D Fermi surface planes at low concentrations.

In this work we observe a hole induced change in the AF structure in a single crystal of $\text{Gd:Y}_{1-x}\text{Ca}_x\text{Ba}_2\text{Cu}_3\text{O}_6$ with a Ca concentration of $x \approx 0.008$. Ca^{2+} substitutes for Y^{3+} and introduces 0.004 holes per $\text{Cu}(2)$ into the AF CuO_2 layers of our sample. We show that in the lightly hole doped AF crystal, holes are not localized in the neighborhood of Ca^{2+} ions down to 2.5 K. We observe AF domains that are static on the time scale of 10^{-8} s at temperatures below 200 K. As opposed to $\text{La}_{2-x}\text{Sr}_x\text{CuO}_4$, $\text{YBa}_2\text{Cu}_3\text{O}_6$ has a tetragonal crystal structure and is therefore sensitive to any small extra anisotropy. We find that the easy axis of sublattice magnetization rotates by 45° as the temperature is lowered. Unlike the undoped reference that has the structure of Fig. 1(a) at all temperatures, in the doped sample the ground state spin orientation is along the diagonal of the CuO_2 square lattice [Fig. 1(b)]. The change of the magnetic anisotropy of the bulk by a very small concentration of holes is an indication of an ordered hole structure.

We use 1% of Gd substituting for Y as a weakly perturbing local electron spin resonance (ESR) probe of the magnetic spin susceptibility and charge redistribution in the AF CuO_2 sandwich. The Gd^{3+} ESR g fac-

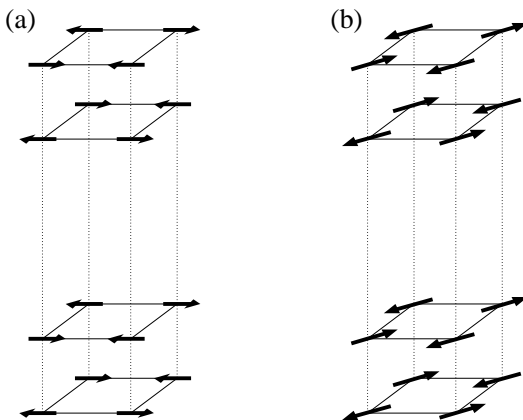


FIG. 1: (a) AFI(0) is the magnetic structure of undoped $\text{YBa}_2\text{Cu}_3\text{O}_6$ at all temperatures below $T_N = 420$ K. (b) AFI($\pi/4$) is the suggested low temperature magnetic structure of $\text{Y}_{1-x}\text{Ca}_x\text{Ba}_2\text{Cu}_3\text{O}_6$.

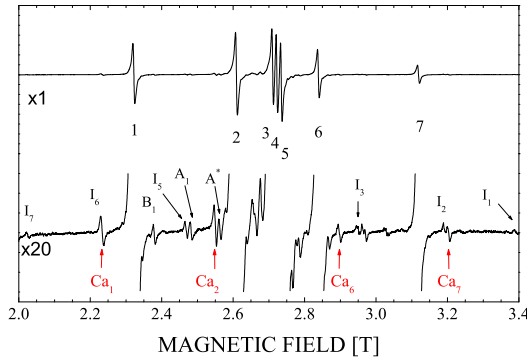


FIG. 2: Assignment of lines in the ESR spectrum of $\text{Gd:Y}_{1-x}\text{Ca}_x\text{Ba}_2\text{Cu}_3\text{O}_6$. “1” to “7”: the main Gd^{3+} fine structure series arise from Gd^{3+} with no Ca^{2+} neighbors. “ Ca_1 ”, “ Ca_2 ”, “ Ca_6 ” and “ Ca_7 ” are the Ca satellite series from Gd^{3+} ions with one first neighbor Ca^{2+} ion. Other lines are independent of Ca doping and are described in the text. $B \parallel c$, $\omega_L/2\pi = 75$ GHz and $T = 18$ K.

tor shifts and zero field splitting (ZFS) parameters are closely related to these quantities. Ref. [9] details the methods used to precisely determine the g factor and the ZFS parameters from the Gd^{3+} ESR fine structure lines. This technique has proven successful in the study of AF $\text{YBa}_2\text{Cu}_3\text{O}_{6+\delta}$ [9, 10] and La_2CuO_4 [11] compounds.

Single crystals of $\text{Gd:Y}_{1-x}\text{Ca}_x\text{Ba}_2\text{Cu}_3\text{O}_6$ and the reference crystal $\text{Gd:YBa}_2\text{Cu}_3\text{O}_6$ were grown in BaZrO_3 crucibles as described elsewhere [12]. The nominal Gd concentration was 1% in agreement with estimates from the intensity of ESR lines from pairs of neighboring Gd^{3+} ions. The nominal Ca concentration was $x_{\text{nom}} = 0.03$, but due to the small distribution coefficient of Ca during crystal growth the actual concentration x determined by atomic absorption spectroscopy (AAS) is much smaller, between 0.005 and 0.01. A Ca concentration of $x = 0.005$ is estimated from the Ca satellite ESR intensity. We shall refer to the Ca concentration as $x = 0.008$.

The ESR spectra testify the high purity of the sample. The powder ESR spectrum of a small amount of a polycrystalline paramagnetic impurity phase (possibly the Y_2BaCuO_5 “green phase”) and the Gd^{3+} fine structure (see Fig. 2) of a low concentration (about 0.5% of the Gd^{3+} ions) of an unidentified Gd site within the single crystal was observed. The X-band ESR spectra of two Ca doped crystals measured at several orientations at 77 K were the same and one crystal of $2 \times 3 \times 0.2$ mm was investigated in detail. The ESR spectra of the reference samples reproduced those reported in Ref. [9] except for a somewhat broader linewidth and a stronger field dependence of the domain structure.

For magnetic field B along the c axis, a single series of strong fine structure lines (main lines) is observed, cor-

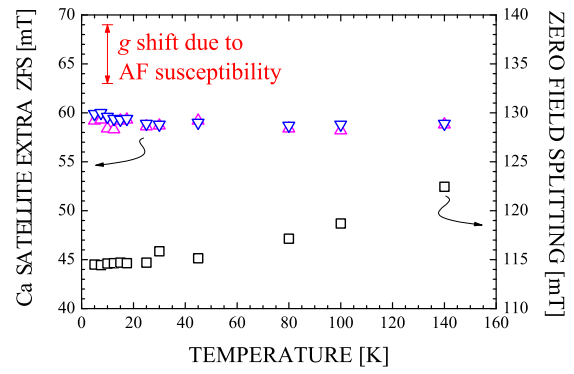


FIG. 3: Left hand scale: “ Ca_2 ” (∇) and “ Ca_6 ” (\square) satellite line positions measured from the corresponding “2” and “6” main lines. The temperature independence of this extra ZFS shows that holes do not localize at Ca^{2+} ions. The g shift caused by the spin susceptibility of the CuO_2 layers (marked by vertical arrow) is equal on the satellite and main lines and is independent of temperature. Right scale: Half distance between main lines “2” and “6”. The temperature dependence is due to lattice expansion.

responding to the majority of Gd^{3+} ions with only Y^{3+} ions occupying the rare earth sites in the neighborhood (Fig. 2). These lines, labeled “1” to “7”, are well fitted by simulated spectra using the same ZFS parameters as for the undoped crystal. Several lines with intensities of the order of 1% of the main lines appear at larger amplification. Most of these were observed in undoped samples also and they are due to closely spaced Gd^{3+} - Gd^{3+} pairs [13] (“ A_1 ”, “ A^* ” and “ B_1 ” in Fig. 2). The unidentified Gd site (series “ I_n ”) has also been observed in previous studies [10].

We assign the satellite lines, “ Ca_1 ”, “ Ca_2 ”, “ Ca_6 ” and “ Ca_7 ”, to Gd^{3+} ions which have a first neighbor rare earth site occupied by a Ca^{2+} ion. (The inner three lines of the series could not be identified.) This series has not been observed in the undoped crystals. The relative intensities, the temperature dependence of the intensities and the Larmor frequency dependence clearly show that these lines belong to a Gd^{3+} fine structure series corresponding to a rare earth site with ZFS parameters not very different from the main line series. The strong first neighbor Ca satellite fine structure series of a magnetically aligned superconducting $\text{Gd:Y}_{0.85}\text{Ca}_{0.15}\text{Ba}_2\text{Cu}_3\text{O}_{6+\delta}$ powder has been easily identified previously [14]. The shifts of the satellites from the main series in the $x = 0.15$ sample are similar to those in the $x = 0.008$ sample studied here.

We first address the question: do the holes localize at low temperatures to the Ca sites or elsewhere? We compare the temperature dependence of the charge distribution and spin susceptibility at sites next to and

distant from Ca^{2+} ions. Gd^{3+} ZFS parameters are highly sensitive to the charge distribution. Doping $\text{Gd:YBa}_2\text{Cu}_3\text{O}_{6+\delta}$ with oxygen from $\delta = 0$ to $\delta = 1$ changes the largest ZFS parameter, b_2^0 , by 40% [15] and changes of this order are expected for the first neighbor Gd^{3+} if holes were to localize to the Ca^{2+} ions within a few lattice constants. Hole localization would then shift the “ Ca_n ” satellite lines on the order of their distances from the central (“4”) line. This is not the case. The observed small, few %, temperature dependence of the ZFS parameters (Fig. 3, squares) is due to thermal expansion of the lattice since the temperature variation is the same at the first neighbors of Ca^{2+} and at sites distant from the Ca^{2+} ions. The extra ZFS caused by the Ca^{2+} neighbor (Fig. 3, triangles), measured by the difference between the “ Ca_2 ” (“ Ca_6 ”) and “2” (“6”) line positions, is temperature independent within $\pm 2\%$ from 2.5 to 140 K. Thus holes do not localize at Ca^{2+} ions (at least above 2.5 K) since the charge redistribution at $\text{Cu}(2)$ and $\text{O}(2)$ lattice atoms surrounding the Ca^{2+} ions would inevitably change the ZFS. Also, the c axis susceptibilities (measured by the g factors) near the Ca site and in the bulk are the same within $\pm 10\%$ in the temperature range of 2.5 to 140 K (Fig. 3) and this reinforces the conclusion that localization of holes does not take place at Ca sites. The equal susceptibilities at the satellite and main sites exclude the possibility that charges are already localized to Ca^{2+} ions at high temperatures.

As shown below, even a light hole doping has a dramatic effect on the magnetic structure. The temperature independent AF domain structure [9, 16] of pristine $\text{YBa}_2\text{Cu}_3\text{O}_6$ was confirmed for the reference sample. The easy direction of the sublattice magnetization \mathbf{M}_s is along $[100]_t$ (any of the equivalent $[100]$ or $[010]$ directions in the tetragonal crystal) in the undoped antiferromagnet. In zero applied field, single crystals are magnetically twinned with equal amounts of domains in the two orthogonal directions, $[100]_t$, of the tetragonal lattice. The domain structure is field dependent, and applying a magnetic field of a few T along a $[100]_t$ direction turns all domains perpendicular to the applied field. In the present reference sample about 80% of domains had \mathbf{M}_s perpendicular to the field in a field of 1 T applied along $[100]_t$.

Nothing is known from experiments about the direction, width, concentration or origin of the domain walls separating the orthogonal domains. Domain walls in the (a, b) plane that separate domains along c were suggested to explain data in undoped crystals [9]. Conducting stripes running along a and separating domains within the (a, b) plane were suggested by Niedermayer *et al.* [17] and Ando *et al.* [18] to explain NMR and magnetoresistance data.

The structure of the ESR lines reflects the distribution of domain orientations. There are two contributions to the Gd^{3+} resonance frequency that depend on the ori-

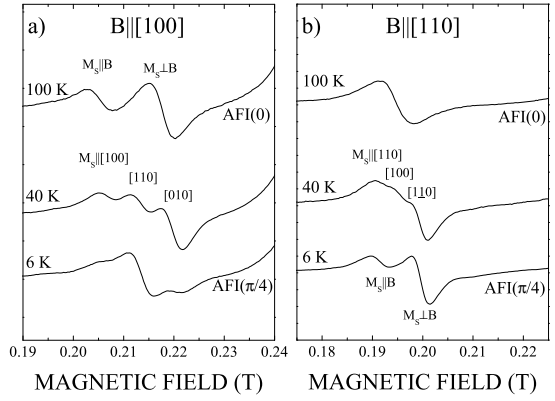


FIG. 4: Magnetic phase transition between $\text{AFI}(0)$ and $\text{AFI}(\pi/4)$ observed in the temperature dependence of a low field Gd^{3+} ESR fine structure line at 9 GHz. The direction of sublattice magnetization \mathbf{M}_s at resolved lines is marked. Magnetic field \mathbf{B} is applied along (a) $[100]$ and (b) $[110]$.

mentation of \mathbf{M}_s : one formally described by a “ g shift” and the other by an orthorhombic ZFS parameter b_2^2 . Most probably, both are due to the exchange interaction J between the CuO_2 planes and Gd^{3+} ions and are proportional to the anisotropic AF spin susceptibility. b_2^2 may also arise from magnetostriction, but the experiments described here suggest that a term second order in J , overlooked in Refs. [9] and [11], is dominant.

The AF domain structure is readily apparent in the Gd^{3+} ESR spectra with magnetic field applied in the (a, b) plane. Fig. 4 displays one component of the fine structure of the 9 GHz ESR spectra at several temperatures for magnetic fields oriented along $[100]_t$ (i.e., magnetic field \mathbf{B} oriented along $\phi_B = 0^\circ$ or 90°) and $[110]_t$ ($\phi_B = 45^\circ$ or 135°). At high temperatures the spectra of the Ca doped and undoped $\text{YBa}_2\text{Cu}_3\text{O}_6$ crystals are similar: the main series are split by the same amount and the line widths are comparable. In contrast to the reference, the ESR spectrum of $\text{Gd:Y}_{1-x}\text{Ca}_x\text{Ba}_2\text{Cu}_3\text{O}_6$ is temperature dependent. A gradual magnetic phase transition is observed around $T_m = 40$ K. Spectra at $T \gg T_m$ and $T \ll T_m$ are qualitatively different. The transition is broad and non trivial changes with temperature are still observed above 85 K and below 15 K. The domain structure and the transition depend on magnetic field. An account of the transition between 0.2 and 5.6 T will be presented elsewhere.

At lower temperatures the magnetic easy axis is rotated by $\pi/4$. Below about 20 K, the ϕ_B dependence of the lines is shifted by $\pi/4$, i.e., the lines in the $\mathbf{B} \parallel [100]_t$ spectrum are similar to the corresponding ones at high temperature in the $\mathbf{B} \parallel [110]_t$ spectrum. We denote the high and low temperature orders as $\text{AFI}(0)$ and $\text{AFI}(\pi/4)$, respectively. The probable cell for $\text{AFI}(\pi/4)$

is shown in Fig. 1(b), but other, larger magnetic cells are also possible. The high temperature spectra are well modeled by the same spin Hamiltonian with the same ZFS parameters as for the undoped case, and this is still true at low temperatures except for a $\pi/4$ rotation of the orthorhombic term b_2^2 .

At high temperatures the system is purely AFI(0) within experimental uncertainties while it is almost purely AFI($\pi/4$) at the lowest temperatures. During the transition the system is inhomogeneous but it is not possible to tell from an analysis of the ESR spectra whether during the phase transition domains rotate continuously or a mixture of the two phases occurs. The lack of hysteresis with cycling the magnetic field and temperature makes a continuous transition more probable.

The AFI(0) to AFI($\pi/4$) phase transition observed here in a high purity, lightly Ca doped crystal has no relation with the AFI(0) to AFII phase transition observed in strongly doped crystals where dopants give rise to magnetic moments in the Cu(1) layer [19, 20]. In the AFII phase every second bilayer is rotated by π and the lattice is doubled along c . This could be easily distinguished from the AFI($\pi/4$) state by ESR.

We believe the transition is related to hole localization in spite of the low hole concentration $p = 0.004$. The sample is of high purity and extrinsic effects are unlikely. The broad temperature range of the magnetic transition (i.e., a continuous change in the distribution of the orientations of \mathbf{M}_s between 100 and 6 K) is consistent with the idea that the magnetic transition is related to the localization of holes. The gradual localization of holes is well documented in Ca doped $\text{YBa}_2\text{Cu}_3\text{O}_6$ [17]. At low temperatures the sublattice magnetization of the bulk becomes the same in hole doped systems as in undoped ones, and for Ca concentrations $x = 0.03$ to 0.06 a broad temperature range of magnetic fluctuations and a magnetic transition to a static order in the range of 10–20 K is observed.

Our findings suggest that in $\text{Y}_{1-x}\text{Ca}_x\text{Ba}_2\text{Cu}_3\text{O}_6$ in analogy to lightly doped $\text{La}_{2-x}\text{Sr}_x\text{CuO}_4$, holes localize into an ordered structure which induces a diagonal spin density wave with spin direction coupled to the propagation vector. The amplitude of the spin density wave is small and the change of the easy axis direction is not accompanied by an observable change of the magnitude of the magnetic susceptibility. However, localized holes change both the direction and the magnitude of the magnetic crystalline anisotropy, since at low temperatures the domain structure persists to high magnetic fields. In the Ca doped sample AF domains are well observed at 5.4 T while they are hardly discernible in the undoped reference at 2.7 T.

It is probable that the easy axis in pristine $\text{YBa}_2\text{Cu}_3\text{O}_6$ is determined by some extrinsic effects, e.g., residual Cu-O chain fragments. This could explain why no change in the easy direction with temperature was observed in

oxygen doped samples [21]. The difference between hole doping by Ca and oxygen is that oxygen chain fragments introduce a local orthorhombic distortion of the structure which at higher concentrations may fix the direction of magnetic crystalline anisotropy at all temperatures.

In conclusion the main result is a new magnetic phase transition in lightly Ca doped $\text{YBa}_2\text{Cu}_3\text{O}_6$ in which the easy direction of the AF sublattice magnetization is rotated by $\pi/4$ in the (a, b) plane. We find that holes do not localize to the Ca dopants suggesting that the transition is related to the condensation of holes into an ordered structure. In view of the similarities of the phase diagrams [17], the diagonal magnetic order in $\text{Y}_{1-x}\text{Ca}_x\text{Ba}_2\text{Cu}_3\text{O}_6$ and the diagonal incommensurate spin modulation observed in doped $\text{La}_x\text{Sr}_{2-x}\text{CuO}_4$ may have a common origin.

We are indebted to Patrik Fazekas and Peter Littlewood for illuminating discussions and to W. Wendl (Universität Karlsruhe) for the AAS analysis. Support of the Hungarian state grants OTKA TS040878, T029150, T043255 and the European Infrastructure Network, SENTINEL, are acknowledged. The work in Lausanne was partly supported by the NCCR research pool “MaNEP” of the Swiss National Science Foundation.

* Electronic address: atj@szfki.hu

- [1] J. M. Tranquada *et al.*, Phys. Rev. Lett. **60**, 156 (1988).
- [2] M. Matsuda *et al.*, Phys. Rev. B **62**, 9148 (2000).
- [3] S. Wakimoto *et al.*, Phys. Rev. B **60**, R769 (1999).
- [4] J. Zaanen, O. Gunnarsson, Phys. Rev. B **40**, 7391 (1989).
- [5] V. J. Emery, S. A. Kivelson, and H. Q. Lin, Phys. Rev. Lett. **64**, 475 (1990).
- [6] J. M. Tranquada *et al.*, Nature **375**, 561 (1995).
- [7] Y. Ando, K. Segawa, S. Komiya, and A. N. Lavrov, Phys. Rev. Lett. **88**, 137005 (2002).
- [8] T. Yoshida *et al.*, preprint, cond-mat/0206469.
- [9] A. Jánossy *et al.*, Phys. Rev. B **59**, 1176 (1999).
- [10] A. Jánossy, A. Rockenbauer, and S. Pekker, Physica C **167**, 301 (1990).
- [11] C. Rettori *et al.*, Phys. Rev. B **47**, 8156 (1993).
- [12] A. Erb, E. Walker, R. Flükiger, Physica C **258**, 9 (1996).
- [13] F. Simon *et al.*, Phys. Rev. B **59**, 12072 (1999).
- [14] A. Rockenbauer, T. Fehér, A. Jánossy, and J. W. Hodby, Proceedings of the 28th Congress Ampere, Kent, UK, 1996.
- [15] A. Rockenbauer, A. Jánossy, L. Korecz, and S. Pekker, J. Magn. Reson. **97**, 540 (1992).
- [16] P. Burlet, J. Y. Henry, and L. P. Regnault, Physica C **296**, 205 (1998).
- [17] Ch. Niedermayer *et al.*, Phys. Rev. Lett. **80**, 3843 (1998).
- [18] Y. Ando, A. N. Lavrov, and K. Segawa, Phys. Rev. Lett. **83**, 2813, (1999).
- [19] H. Kadowaki *et al.*, Phys. Rev. B **37**, 7932 (1988).
- [20] E. Brecht *et al.*, Phys. Rev. B **56**, 940 (1997).
- [21] H. Casalta *et al.*, Phys. Rev. B **50**, 9688 (1994).